INSTITUTE OF PHYSICS PUBLISHING PHYSICAL BIOLOGY
Phys. Biol. **2** (2005) 29–35 doi:10.1088/1478-3967/2/1/004

Dynamic behaviour of the B_{12} riboswitch

Moisés Santillán[1,2] **and Michael C Mackey**[2,3]

[1] Departamento de Física, Escuela Superior de Física y Matemáticas, Instituto Politécnico Nacional, Edificio 9, U. P. Zacatenco, 07738 México DF, Mexico
[2] Centre for Nonlinear Dynamics, McGill University, 3655 Promenade Sir William Osler, H3G 1Y6 Montreal, QC, Canada
[3] Departments of Physiology and Physics and Mathematics, McGill University, Montreal, QC, Canada

E-mail: moyo@esfm.ipn.mx and mackey@cnd.mcgill.ca

Received 18 December 2004
Accepted for publication 8 February 2005
Published 2 March 2005
Online at stacks.iop.org/PhysBio/2/29

Abstract
Riboswitches are RNA segments that serve as ligand-responsive genetic control elements. They modulate the expression of certain genes in response to changing concentrations of metabolites. In this paper, we study the dynamic behaviour of the B_{12} riboswitch in *E. coli*—perhaps the most widely studied and best known of all riboswitches—through a mathematical model of its regulatory pathway. To carry this out, we simulate dynamic experiments in which the bacterial B_{12} uptake capacity is measured after being depleted of this vitamin for a long time. The results of these simulations compare favourably with reported experimental data. The model also predicts that an overshoot of intracellular B_{12} should be observed if the replenishment experiments were to be carried out for longer times. This behaviour is discussed in terms of a possible evolutionary advantage for *E. coli*, together with the fact that regulation at the transcriptional and translational levels is almost equivalent dynamically.

1. Introduction

After the introduction of the *operon* concept by Jacob and Monod in the early 1960s [1] it was initially thought that regulation of gene expression always involved proteins that sense the presence of a small molecule, such as a hormone or amino acid, and then bind DNA or RNA. This picture has slowly evolved, and the recent discovery of riboswitches is contributing to our dramatically changing understanding of gene regulation. An excellent review of riboswitches can be found in [2].

Riboswitches are RNA segments that serve as ligand-responsive genetic control elements. They modulate the expression of certain genes in response to changing concentrations of metabolites. Riboswitches are typically embedded within the 5′-untranslated region of specific prokaryotic mRNAs, and are composed of two functional and sometimes distinct structural domains. One domain serves as a natural *aptamer* that binds the target metabolite with high selectivity. The other domain is an *expression platform* that harnesses allosteric changes in RNA structure, brought about by aptamer–metabolite complex formation, to control expression of the adjacent gene or operon. In prokaryotes, expression platforms have been identified that control transcription termination or translation.

To date, seven fundamental metabolites are known to be detected by riboswitches. These targets include the nucleobases guanine and adenine, the amino acid lysine, and the coenzymes thiamine pyrophosphate, FMN (flavin mononucleotide), SAM (S-adenosylmethionine) and B_{12} (adenosylcobalamin or AdoCbl). Several classes of riboswitches have been shown by database searches to be distributed widely among prokaryotic organisms, and some examples have been identified in archeans. Sequence variants of the natural aptamer for thiamine pyrophosphate also have been identified in certain fungal and plant mRNAs, where they bind the coenzyme with affinities that match those of their prokaryotic counterparts. These findings indicate that riboswitches are a fundamental and widespread form of genetic control.

The taxonomic diversity of genomes containing riboswitches and the diversity of molecular regulatory mechanisms, in conjunction with the fact that direct interaction of riboswitches with their effectors does not require additional factors, suggest that riboswitches represent one of the oldest regulatory systems. This is consistent with the so-called *RNA*

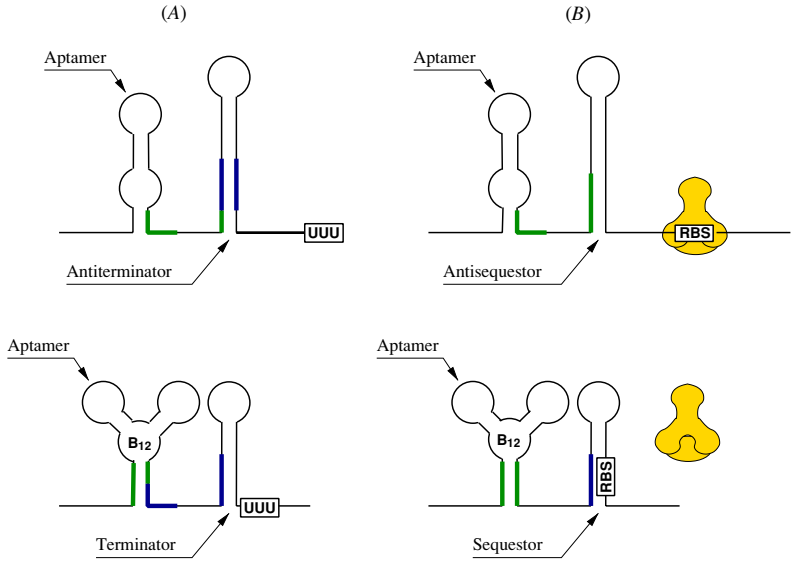

Figure 1. Schematic representation of the two control mechanisms observed in the B_{12} riboswitch. (*A*) Regulation at the transcriptional level. The binding of a B_{12} to the aptamer induces formation of a terminator stem that causes RNA polymerase to abort transcription before the coding portion of the mRNA has been made. (*B*) Regulation at the translational level. The binding of a B_{12} molecule to the aptamer induces an allosteric change in the expression platform that sequesters the ribosome binding site (RBS) and avoids translation initiation. It must be realized that the actual mRNA folding is more complex than that shown here. Nevertheless, the overall riboswitch-regulation picture presented in this scheme is accurate.

world hypothesis, according to which there was a period in the early biosphere when both the information needed for life and the enzymatic activity of living organisms were contained in RNA molecules [3, 4].

In the case of the coenzyme-B_{12} riboswitch, two main mechanisms for gene control are apparent. Below, they are described in detail. A schematic depiction of these two control mechanisms can be found in figure 1.

The first control mechanism in the B_{12} riboswitch regulates RNA transcription and involves the ligand-dependent formation of an intrinsic terminator stem. Intrinsic terminators are extended stem–loop structures, typically followed by a run of six or more U residues that cause RNA polymerase to abort transcription before the coding portion of the mRNA has been made. When coenzyme B_{12} is not present in sufficient quantities, transcription of an mRNA associated with the coenzyme-B_{12} riboswitch produces a nascent mRNA wherein the aptamer domain remains uncomplexed with the ligand. The unbound aptamer domain permits formation of an antiterminator stem, which precludes formation of the intrinsic terminator stem and thereby permits transcription of the complete mRNA. However, when coenzyme-B_{12} concentrations are adequate, the nascent mRNA binds to a coenzyme-B_{12} molecule and the allosteric change in structure permits the intrinsic terminator stem to form. Transcription termination results, and gene expression is prevented because the coding region of the mRNA is not made.

The second mechanism used by the coenzyme-B_{12} riboswitch functions at the level of translation initiation. Coenzyme-B_{12} binding causes structural changes in full-length mRNAs to control access to the ribosome binding site. Specifically, it has been shown that ribosomes are not able to form stable complexes with the *btuB* mRNA of *E. coli* when coenzyme B_{12} is present. In rare instances, it appears that both transcription and translation can be controlled simultaneously. This would be possible if the transcription-terminator stem is formed by including base pairing with the ribosome-binding site. This combination of mechanisms would allow newly initiated mRNA transcripts to be aborted by the terminator stem, whereas transcripts whose synthesis had already passed the point of transcription termination could exploit the same structural change to prevent translation by occluding the ribosome-binding site.

2. A mathematical model for the B_{12} riboswitch in *E. coli*

E. coli is incapable of synthesizing vitamin B_{12}. Instead, these bacteria actively transport the vitamin from the environment. Protein BtuB, which is encoded by gene *btuB*, is an important component of the vitamin B_{12} transporter. Gene *btuB* is negatively regulated by vitamin B_{12} via a riboswitch. This riboswitch is capable, in principle, of regulating *btuB* expression at both the transcriptional and the translational level [2]. Regulation at the transcriptional level occurs when a B_{12} molecule binds the riboswitch aptamer domain and causes the formation of a terminator structure in the riboswitch expression platform. Transcription is prematurely terminated shortly after it is started. Regulation at the translational level also occurs when a B_{12} molecule binds the riboswitch aptamer domain, inducing the formation of a secondary structure in the expression platform. This secondary structure sequesters the ribosome binding site, preventing transcription initiation.

To develop a mathematical model for the B_{12}-riboswitch regulatory network in *E. coli*, we identify three model variables

by M, E and P, which respectively stand for the concentration of *btuB* mRNA, the concentration of protein BtuB, and the concentration of vitamin B_{12}. The model itself is framed in three differential equations:

$$\dot{M} = \alpha\Phi(P) - \gamma M, \tag{1}$$

$$\dot{E} = \beta M\Theta(P) - \xi E, \tag{2}$$

$$\dot{P} = \zeta(P_{\text{ext}})E - \delta P. \tag{3}$$

The constants α, β, γ, ξ and δ are all positive, and respectively denote the *btuB*-promoter transcription initiation rate, the *btuB*-mRNA translation initiation rate, and the mRNA, BtuB, and B_{12} degradation-plus-dilution rates. $\zeta(P_{\text{ext}})$ is the B_{12} transport rate per unit BtuB concentration. Since B_{12} is actively transported, ζ is a monotonic increasing function of the external B_{12} concentration, P_{ext}, such that $\zeta(0) = 0$ and $\lim_{P_{\text{ext}}\to\infty}\zeta(P_{\text{ext}}) = \zeta_{\max}$. The functions $\Phi(P)$ and $\Theta(P)$ denote the B_{12}-governed regulation at the transcriptional and translational levels respectively. In appendix A these functions are shown to be given by the following Michaelis–Menten equations:

$$\Phi(P) = \frac{K_\phi}{K_\phi + P}, \tag{4}$$

$$\Theta(P) = \frac{K_\theta}{K_\theta + P}. \tag{5}$$

A linear loss rate for the concentration of B_{12} (P) is assumed because it is a coenzyme, and thus is not degraded after entering a biochemical pathway.

3. Steady state

The steady state of the model described by equations (1)–(3) is defined by the condition $\dot{M} \equiv \dot{E} \equiv \dot{P} \equiv 0$, and the steady state will be denoted by (M_*, E_*, P_*). After solving for M from equation (1) with $\dot{M} = 0$, substituting the result into the steady-state version of equation (2), and solving for E_* we obtain

$$E_* = \frac{\alpha\beta}{\gamma\xi}\Phi(P_*)\Theta(P_*). \tag{6}$$

Also solving for E_* in the steady-state version of equation (3) yields

$$E_* = \frac{\delta}{\zeta(P_{\text{ext}})}P_*. \tag{7}$$

From equations (6) and (7) the steady-state values for the variable P are given by the roots of the equation

$$\Phi(P_*)\Theta(P_*) = \frac{\xi\gamma\delta}{\alpha\beta\zeta(P_{\text{ext}})}P_*. \tag{8}$$

Since the left-hand side of equation (8) is a monotone decreasing function of P_* (Φ and Θ are both monotone decreasing functions), while the right-hand side is a linearly increasing function of P_*, this equation has a unique positive real root and the system has a single steady state. Moreover, the slope of the straight line determined by the right-hand side of equation (8) decreases as P_{ext} increases. Hence, P_* is a monotone increasing function of P_{ext} and its maximum value $P_{\max}$ is given by the solution of

$$\Phi(P_{\max})\Theta(P_{\max}) = \frac{\xi\gamma\delta}{\alpha\beta\zeta_{\max}}P_{\max}. \tag{9}$$

More specifically, the function $P_*(P_{\text{ext}})$ is such that $P_*(0) = 0$ and $\lim_{P_{\text{ext}}\to\infty}P_*(P_{\text{ext}}) = P_{\max}$.

Once the value of P_* is known, the steady-state values of the other two variables can be calculated by means of equation (7) and

$$M_* = \frac{\alpha}{\gamma}\Phi(P_*). \tag{10}$$

The last equation results from solving for M in the steady-state version of equation (1).

4. Parameter estimation

To compare the behaviour of this model with existing experimental data, we must estimate the parameters appearing in equations (1) through (3). To do this effectively it is convenient to make the concentrations appearing in these equations dimensionless; we normalize M, E and P to the maximum possible steady-state values they can reach, denoting these maximum values by $M_{\max}, E_{\max}$ and $P_{\max}$. Thus, the corresponding dimensionless variables are $m = M/M_{\max}$, $e = E/E_{\max}$ and $p = P/P_{\max}$.

To determine these maximum normalizing values, first note that $\Phi(P)$ and $\Theta(P)$ approach 1 as $p \to 0$. From this it immediately follows that

$$M_{\max} = \frac{\alpha}{\gamma} \qquad \text{and} \qquad E_{\max} = \frac{\alpha\beta}{\gamma\xi},$$

so

$$\dot{m} = \gamma[\phi(p) - m], \tag{11}$$

$$\dot{e} = \xi[m\theta(p) - e], \tag{12}$$

$$\dot{p} = \delta[\epsilon(P_{\text{ext}})e - p], \tag{13}$$

where

$$\phi(p) = \frac{(K_\phi/P_{\max})}{(K_\phi/P_{\max}) + p},$$

$$\theta(p) = \frac{(K_\theta/P_{\max})}{(K_\theta/P_{\max}) + p},$$

$$\epsilon(P_{\text{ext}}) = \frac{\alpha\beta}{\gamma\xi\delta P_{\max}}\zeta(P_{\text{ext}}) = \frac{1}{\phi(p_*(P_{\text{ext}}))\theta(p_*(P_{\text{ext}}))},$$

with $p_*(P_{\text{ext}}) = P_*(P_{\text{ext}})/P_{\max}$. From its definition and the properties of P_* it follows that $p_*(0) = 0$ and $\lim_{P_{\text{ext}}\to\infty}p_*(P_{\text{ext}}) = 1$. Since $\epsilon(P_{\text{ext}}) \propto \zeta(P_{\text{ext}})$ it is easy to show that $\epsilon(P_{\text{ext}})$ is a monotone increasing function of P_{ext}, $\epsilon(0) = 0$ and $\lim_{P_{\text{ext}}\to\infty}\epsilon(P_{\text{ext}}) = \epsilon_{\max} = 1/\phi(1)\theta(1)$.

Nou and Kadner [5] studied *btuB–lacZ* fusions at both the transcriptional and translational levels. From their results, the modulation of translational fusions (including both transcriptional and translational regulation) under conditions

of excess external B_{12} can reach at least 25 times that corresponding to the steady-state value in which $P_{\text{ext}} = 0$. Meanwhile the modulation of transcriptional fusions (including only transcriptional regulation) under conditions of large P_{ext} values is about 5 times the steady-state level corresponding to zero P_{ext}. From this we conclude that $\phi(1) = \theta(1) = 1/5$. Thus, $K_\phi/P_* = K_\theta/P_* = 1/4$. Moreover, $\epsilon_{\max} \simeq 25$ and we can write

$$\phi(p) = \theta(p) = \frac{K}{K+p},$$

where $K = K_\phi/P_* = K_\theta/P_* = 1/4$.

The growth rate of *E. coli* cultured in a minimal medium is $\mu \simeq 0.8 \times 10^{-2}$ min^{-1} [6]. From [5], the *btuB*-mRNA half-life is about 11 min. Thus its degradation rate is about $\ln(2)/11$ min $\simeq 6.3 \times 10^{-2}$ min^{-1}, and $\gamma \simeq (0.8 + 6.3) \times 10^{-2}$ min^{-1} $\simeq 7.1 \times 10^{-2}$ min^{-1}. Here, we assume that the BtuB degradation rate is negligible, and so $\xi \simeq \mu \simeq 0.8 \times 10^2$ min^{-1}. B_{12} is highly unstable under ambient light conditions. Indeed, Nahvi *et al* [7] measured a degradation rate for light-exposed vitamins of the order of $\delta \simeq 3.6$ min^{-1}. However, the value of δ is estimated in the next section by fitting the model to dynamic experiments reported in the literature, carried out with wild-type bacterial strains. The result of this estimation is $\delta \simeq 0.8$ min^{-1}.

Parameters γ, ξ and δ determine how fast the dynamics of m, e and p are —see equations (11)–(13). From the estimations in the previous paragraphs it follows that γ is one order of magnitude larger than ξ and δ. This fact implies, on the one hand, that the dynamics of m are much faster than those of e and p. On the other hand, it also justifies a quasi-steady-state assumption for the equation governing the dynamics of m. Making this quasi-steady-state assumption by taking $\dot{m} = 0$ in equation (11), solving for m, and substituting into equation (12), leads to the following simplified model for the B_{12} riboswitch:

$$\dot{e} = \xi[\phi(p)\theta(p) - e], \tag{14}$$

$$\dot{p} = \delta[\epsilon(P_{\text{ext}})e - p]. \tag{15}$$

5. Comparison with experiments that measure the temporal evolution of vitamin B_{12} replenishment

Gudmundsdottir *et al* [8] carried out experiments to measure the time course of B_{12} uptake in *E. coli* cultures with insertion mutations in the *btuB* gene. The *btuB* gene was mutated by the insertion of 6-base pair linkers into each of ten *HpaII* sites distributed throughout the coding region. Receptor function was measured with the mutated genes present in single or multiple copies. The bacterial capacity for transporting B_{12} from the environment was measured by adding a large amount of this vitamin to the growth medium, after culturing the bacteria in so-called minimal medium, and recording the amount of intracellular B_{12} at different times. For the purpose of the present work we shall call the Gudmundsdottir *et al* experiments B_{12} replenishment experiments.

To simulate the Gudmundsdottir *et al* experiments the model equations (11)–(13) were numerically solved with the following set of initial conditions: $m = 1$, $e = 1$ and $p = 0$. These initial conditions are most likely to correspond to the situation of a bacterial culture that has grown for a long time in a B_{12}-free medium. To compare with the wild-type-strain experiments we set $\epsilon(P_{\text{ext}}) = \epsilon_{\max} = 25$ at $t = 0$, to simulate the high B_{12} dose given to the bacterial culture. Then the value of parameter δ was chosen so that the simulated p versus t curve fits the experimental points. The minimum value allowed for this parameter, $\delta \simeq \mu \simeq 0.8 \times 10^{-2}$ min^{-1} (corresponding to a negligible degradation rate) was found to give a good fit to the data. This value of δ justifies the quasi-steady-state assumption for $\dot{m}$ and leads to the simplified model given by equations (14) and (15). The replenishment experiment corresponding to the wild-type strain was once more simulated with the simplified model. For this, the following initial conditions were employed: $e = 1$ and $p = 0$. The results obtained with these assumptions support the validity of the quasi-steady assumption.

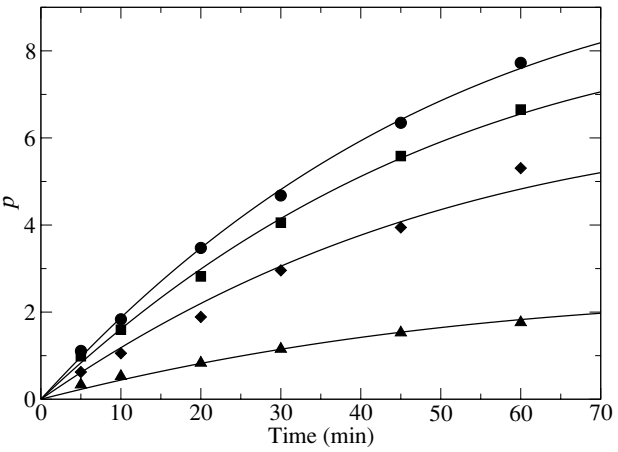

Figure 2. Comparison of the Gudmundsdottir *et al* experimental data and the model simulations. The experimental points corresponding the wild-type, 375, 434 and 343 strains are respectively represented with circles, squares, diamonds and triangles. The values of ϵ employed in these simulations are as follows: $\epsilon = 25$ (wild-type strain), $\epsilon = 21.5$ (375 mutant strain), $\epsilon = 15.75$ (434 mutant strain), and $\epsilon = 5.8$ (343 mutant strain).

Data from the mutant stains used by Gudmundsdottir *et al* were simulated with the simplified model by decreasing the value of ϵ while keeping the estimated value of δ fixed. Recall that $\epsilon \propto \zeta$ and thus ϵ is related to the bacterial B_{12} uptake capacity. Since the induced mutations reduce this uptake capability, the natural choice is to simulate them by decreasing ϵ.

The simulations of the Gudmundsdottir *et al* experiments are shown in figure 2. Since the model variables are normalized, the experimental values of the B_{12} concentration points are rescaled to compare with the model simulation. The model reproduces the time course of the wild-type and mutant-strain experiments quite well, and it is important to realize that this fit of the model to the data is achieved solely with the change of one parameter.

In the wild-type experiment, the intracellular B_{12} level reaches much higher values than the expected $p_* = 1$ steady-state value. A similar conclusion holds for the mutant-strain

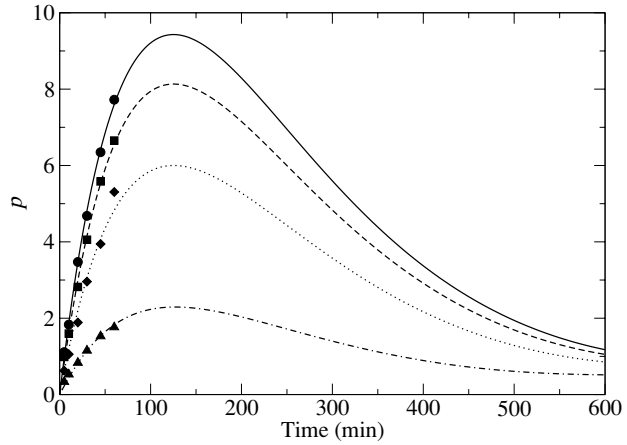

Figure 3. Simulations of B_{12} replenishment experiments carried out for much longer times than those of figure 2. The solid, dashed, dotted and dash–dotted lines respectively correspond to $\epsilon = 25$, $\epsilon = 21.5$, $\epsilon = 15.75$ and $\epsilon = 5.8$. Note that the B_{12} levels undergo an overshoot before reaching their steady-state value. The corresponding available experimental points are also shown.

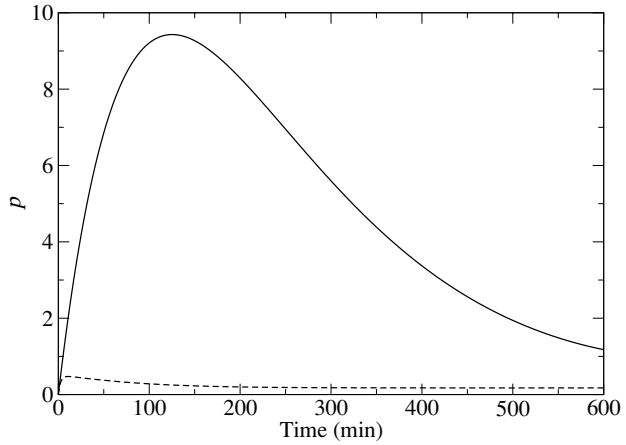

Figure 4. Simulations of B_{12} replenishment experiments. The solid line corresponds to a bacterial strain, while the dashed line corresponds to a bacterial strain growing under conditions such that the B_{12} degradation rate is increased to 50 times normal. In both cases $\epsilon = 25$.

experiments. This observation can be appreciated by plotting the p versus t curves for longer times, as in figure 3. In all cases, the predicted B_{12} level undergoes an overshoot before reaching its steady state. This is an important prediction of the model that can be tested experimentally. It is important to note at this point that no other combination of parameters ξ and δ (obeying the restriction $\xi, \delta \geqslant \mu$) allows the model to reproduce the Gudmundsdottir *et al* experimental data. Therefore, if the model is correct, the predicted overshoot should be experimentally observed by recording the intracellular B_{12} values for longer times.

6. Further results

Of the many molecular systems controlled by the B_{12} riboswitch, some are regulated at either the transcriptional or the translational level, while others include both regulation types [2]. The present model can be modified to account only for transcriptional regulation by setting $\phi = \kappa/(\kappa + p)$ and $\theta = 1$. The value of κ is set equal to $1/24$ so that the extent of regulation is the same as in the original model; that is, $e_*(\epsilon = 1) = e_*(\epsilon = 0)/25$. Similarly, to modify the model so that it accounts for regulation only at the translational level we set $\phi = 1$ and $\theta = \kappa/(\kappa + p)$. Simulations (not shown) carried out with the full and with the modified models follow a very similar time course. Indeed, the simulations corresponding to the modified models that account only for either transcriptional or translational regulation are practically indistinguishable from those corresponding to the full model. This can be understood by noting that both ϕ and θ appear as multiplicative terms in equation (14) and thus, from a dynamical point of view, it is not really important whether regulation takes place at the transcriptional, translational, or both levels.

These results imply that having either one or both regulatory mechanisms is dynamically almost equivalent. Interestingly, all three possibilities (only transcriptional regulation, only translational regulation, or both) have been observed experimentally. If one of these combinations presented a clear dynamic advantage over the others, one would expect it to be predominant. The noise inherent to molecular system is another important issue. It is possible that noise control is more efficiently performed by one of the combinations of regulatory mechanisms and thus, it would be more advantageous. Further studies (both experimental and theoretical) are necessary to explore this and other important issues concerning riboswitch dynamics.

The overshoot in B_{12} levels predicted in the simulations and shown in figure 3 are most intriguing. An exhaustive search in the $\xi - \delta$ parameter space led us to the conclusion that the dynamic experimental results of Gudmundsdottir *et al* can be reproduced only with the ξ and δ ($\xi, \delta \geqslant \mu$) values reported in sections 4 and 5. Thus, if the model captures the essential dynamic features of the B_{12} riboswitch in *E. coli*, it predicts the existence of a large and long-lasting overshoot. This prediction could be easily tested experimentally by recording the concentration of B_{12} for much longer times than in experiments like those of Gudmundsdottir *et al*.

We believe that the predicted overshoot in B_{12} levels, during a replenishment experiment, may be biologically significant since it could represent a defence mechanism against a sudden increase of the B_{12} degradation rate. Recall that this vitamin is highly stable in the absence of light but, when illuminated, its degradation rate increases more than 300 times [7]. In figure 4 simulations of the Gudmundsdottir *et al* experiments are shown under normal conditions and with the B_{12} degradation rate increased to 50 times normal. Note that in the second case, the concentration of B_{12} reaches its maximum value (which is approximately equal to its normal steady-state value, $p_* \simeq 1$) in less than 20 min after the vitamin addition and then, decays slowly to its corresponding steady-state value. The decay after the overshot maximum is so slow that the

conditions that caused the B_{12} degradation rate increment may well disappear before the B_{12} concentration reaches very low values and the bacteria are seriously affected.

7. Conclusion and outlook

The current explosion of genomic data threatens the capability of experimentalists to integrate this knowledge into comprehensive models of the corresponding biological systems. The term *systems biology* has been coined to identify a new branch of science whose ultimate goal is to understand the functioning of tissues, organs and organisms from their genome [9]. Given the extreme complexity of even a single eukaryotic cell, the only feasible path for systems biology is to develop methods for studying subsystem networks, over subsystem timescales, the complexity of which might be addressable. The task of systems biology is not to build the system from is molecular components, but to build subsystems from molecules, and then the system from these subsystems.

The dynamic role of riboswitches in the context of systems biology appears to be essential. Bioinformatics has been dedicated, in part, to reconstructing complex gene networks from the transcription factors involved in the control of genes. However, the existence of riboswitches demonstrates that consideration of transcription factors alone is not enough to understand gene regulation. The solution of this riddle will necessarily involve experimental and modelling efforts at different levels. A first step in this approach could be to elaborate detailed mathematical models of the simplest and best known riboswitches, with the objective of gaining insight into their dynamic behaviour, and developing adequate mathematical and modelling techniques. Further steps would involve dealing with other and more complex gene networks.

The model of the B_{12} riboswitch introduced in the present paper is but one attempt in this direction. Interestingly, it raises a few important questions. Does the overshoot in the B_{12} level predicted during a replenishment experiment really exist? Does the overshoot provide *E. coli* with any adaptive advantage? What are the advantages and disadvantages of regulating the riboswitch at the transcriptional or translation levels? At both levels? In section 6 we discussed some preliminary answers to these questions. More experimental work is required before definitive answers will be available. In particular, we believe that carrying out replenishment experiments for longer times, under different light conditions, and with bacterial strains in which this riboswitch is subject to either transcriptional or translational regulation may be useful.

Finally, we wish to point out a few general issues concerning riboswitches that we feel can and will be answered by a combination of experimental and mathematical work:

- Riboswitch B_{12} is negatively regulated; that is, a high metabolite (B_{12}) concentration decreases the activity of the genes controlled by this riboswitch. Many other riboswitches are negatively regulated. However, there also exist a few subject to positive control [2]. It is known that positively regulated systems may exhibit features such as multistability [10]. Is this the case in some riboswitches? If so, what is its biological meaning?
- According to our model, there is no appreciable difference between regulation at the transcriptional and translational levels in riboswitch B_{12}. Whether this property is shared by other riboswitches and what its biological significance might be, are questions that deserve further attention.
- Deterministic models, like the present one, provide accurate results for bacterial cultures. However, this is not the case for single cells. The reason is to be found in the small number of molecules involved in most reactions (from one or two, to a few thousands). This results in large fluctuations around the molecule-count time-course predicted by deterministic models. Since the number of mRNA molecules is usually much smaller than the enzyme level, intrinsic fluctuations affect transcriptional regulation more than they affect translational regulation. How important this fact is for riboswitch regulation is a question that can be explored both experimentally and through mathematical models like in [11].

Acknowledgments

This work was supported by COFAA-IPN (México), EDI-IPN (México), CONACyT (México), MITACS (Canada) and the Natural Sciences and Engineering Research Council (NSERC grant OGP-0036920, Canada).

Appendix A. Regulation at the transcriptional and translational levels

In the B_{12} riboswitch regulated at the transcriptional level the section of the nascent mRNA known as the aptamer is bound by a B_{12} molecule. This further induces formation of a terminator stem that causes RNA polymerase to abort transcription before the coding portion of the mRNA has been made. It follows from these considerations that the production rate of complete mRNA is proportional to the probability that the aptamer is not bound by a B_{12} molecule.

Let A, P and A_P respectively denote the aptamer, a B_{12} molecule, and the aptamer–B_{12} complex. The reaction through which a B_{12} molecule binds the aptamer is

$$A + P \overset{K_\phi}{\rightleftharpoons} A_P.$$

The equilibrium equation for this reaction is

$$AP = K_\phi A_P.$$

Furthermore, the total aptamer concentration is conserved; that is,

$$A + A_P = A_{\text{tot}}.$$

From the last two equations, the following expression for the fraction of free aptamers can be derived after a little algebra:

$$\Phi(P) = \frac{A}{A_{\text{tot}}} = \frac{K_\phi}{K_\phi + P}.$$

In conclusion, the complete-mRNA production rate in a riboswitch subject to regulation at the transcriptional level is proportional to $\Phi(P)$.

In the B_{12} riboswitch regulated at the translational level, the binding of a B_{12} molecule to the aptamer induces an allosteric change in the expression platform that sequesters the ribosome binding site and avoids translation initiation. Thus the rate of transcription initiation is proportional to the probability that the aptamer is not bound by a B_{12} molecule. Thus, following the same procedure as in the case of transcriptional regulation, the translation initiation rate in a riboswitch subject to regulation at the translational level is proportional to

$$\Theta(P) = \frac{A}{A_{\mathrm{tot}}} = \frac{K_\theta}{K_\theta + P},$$

where K_θ is the dissociation constant of the reaction by means of which a B_{12} molecule binds the aptamer.

Glossary

Riboswitch. Riboswitches are RNA segments that serve as ligand-responsive genetic control elements. They modulate the expression of certain genes in response to changing concentrations of metabolites.

Riboswitch B_{12}. *E. coli* is unable to synthesize vitamin B_{12} and has to actively transport it from the environment. Riboswitch B_{12} controls the gene coding for protein BtuB, which is one of the components of the vitamin-B_{12} transporter. In this riboswitch, vitamin B_{12} is the metabolite that binds the aptamer to regulate gene *btuB*.

Aptamer. Riboswitches are composed of two functional and sometimes distinct structural domains. The first domain is known as the aptamer and binds the target metabolite with high selectivity.

Expression platform. The second domain of riboswitches is the expression platform. It harnesses allosteric changes in RNA structure, brought about by aptamer–metabolite complex formation, to control expression of the adjacent gene or operon.

Terminator. In riboswitches regulated at the transcriptional level, formation of the aptamer–metabolite complex induces a structure in the expression platform that prematurely aborts transcription: thus the terminator.

Antiterminator. When the aptamer is not bound by a metabolite, a structure in the expression platform that precludes the terminator is formed: the antiterminator.

Sequestor. In riboswitches regulated at the translational level, formation of the aptamer–metabolite complex induces a structure in the expression platform that sequesters the ribosome binding site to prevent translation initiation: the sequestor.

Antisequestor. When the aptamer is not bound by a metabolite, a structure in the expression platform that precludes the sequestor is formed: the antisequestor.

References

[1] Beckwith J 1996 *Escherichia coli and Salmonella thyphymurium: Cellular and Molecular Biology* vol 2, ed F C Neidhart, R Curtis, J L Ingraham, E C C Lin, K B Low, B Magasanik, W S Reznikoff, M Riley, M Schaechter and H E Umbarger (Washington, DC: ASM) pp 1553–69

[2] Mandal M and Breaker R R 2004 *Nat. Rev. Mol. Cell Biol.* **5** 451–63

[3] Gilbert W 1986 *Nature* **319** 618

[4] Joyce G F 2002 *Nature* **418** 214–21

[5] Nou X and Kadner R J 1998 *J. Bacteriol.* **180** 6719–28

[6] Bremmer H and Dennis P P 1996 *Escherichia Coli and Salmonella Thyphymurium: Cellular and Molecular Biology* vol 2 ed F C Neidhart, R Curtis, J L Ingraham, E C C Lin, K B Low, B Magasanik, W S Reznikoff, M Riley, M Schaechter and H E Umbarger (Washington D C: ASM) pp 1527–42

[7] Nahvi A, Sudarsan N, Ebert M S, Zou X, Brown K L and Breaker R R 2002 *Chem. Biol.* **9** 1043–9

[8] Gudmundsdottir A, Bradbeer C and J K R 1998 *J. Biol. Chem.* **263** 14224–30

[9] Marshall A 2004 *Nat. Biotechnol* **22** 1191

[10] Laurent M and Kellershohn N 1999 *Trends. Biochem. Sci.* **24** 418–22

[11] Swain P S, Elowitz M B and Siggia E 2002 *Proc. Natl Acad. Sci. USA* **99** 12795–800